Computers, Materials & Continua

Tech Science Press

DOI: 10.32604/cmc.2023.036729
Article

Quasi-Phase Equilibrium Prediction of Multi-Element Alloys Based on Machine Learning and Deep Learning

Changsheng Zhu[1,2,*], Borui Zhao[1], Naranjo Villota Jose Luis[1], Zihao Gao[1] and Li Feng[3]

[1]College of Computer and Communication, Lanzhou University of Technology, Lanzhou, 730050, China
[2]State Key Laboratory of Gansu Advanced Processing and Recycling of Non-Ferrous Metal, Lanzhou University of Technology, Lanzhou, 730050, China
[3]College of Materials Science and Engineering, Lanzhou University of Technology, Lanzhou, 730050, China
*Corresponding Author: Changsheng Zhu. Email: zhucs_2008@163.com
Received: 10 October 2022; Accepted: 29 December 2022; Published: 09 June 2023

Abstract: In this study, a phase field model is established to simulate the microstructure formation during the solidification of dendrites by taking the Al-Cu-Mg ternary alloy as an example, and machine learning and deep learning methods are combined with the Kim-Kim-Suzuki (KKS) phase field model to predict the quasi-phase equilibrium. The paper first uses the least squares method to obtain the required data and then applies eight machine learning methods and five deep learning methods to train the quasi-phase equilibrium prediction models. After obtaining different models, this paper compares the reliability of the established models by using the test data and uses two evaluation criteria to analyze the performance of these models. This work find that the performance of the established deep learning models is generally better than that of the machine learning models, and the Multilayer Perceptron (MLP) based quasi-phase equilibrium prediction model achieves the best performance. Meanwhile the Convolutional Neural Network (CNN) based model also achieves competitive results. The experimental results show that the model proposed in this paper can predict the quasi-phase equilibrium of the KKS phase-field model accurately, which proves that it is feasible to combine machine learning and deep learning methods with phase-field model simulation.

Keywords: Deep learning; machine learning; quasi-phase equilibrium; material simulation

1 Introduction

Multicomponent alloy is the most common practical metal material in industrial production. The solidification of alloy is the basis of subsequent reprocessing steps, and it is significant to recognize the formation process of microstructure for the industrial production of the alloy. Dendrite, a typical structure of solidification microstructure, its growth process and the morphological evolution need to be analyzed in detail [1]. As a research method developed rapidly in recent years, numerical simulation

has the advantages of low experimental cost, fewer operating restrictions and simple experiment reproduction, which becomes a meaningful way to analyze solidification microstructure.

There are many methods for numerical simulation of microstructure during alloy solidification. Sun et al. [2] established a two-dimensional model based on Lattice Boltzmann (LB) to simulate the dendrite growth of binary alloy under forced convection. The results show that convection would affect solute distribution strongly and lead to asymmetric dendrite growth. Eshraghi et al. [3] proposed a three-dimensional parallel model combining Lattice Boltzmann and Cellular Automata methods called LB-CA and simulated the microstructure of binary alloy by this model. The simulation achieved appreciable accuracy. Chen et al. [4] simulated the dendrite growth of ternary alloy by using a three-dimensional CA model and researched the secondary dendrite arm spacing in dendrite growth process. Sakane et al. [5] used the three-dimensional Phase Field-Lattice Boltzmann Method (PF-LBM) model to simulate the large-scale dendrite growth under the melt flow. Zhang et al. [6] applied the CA-LBM model with dynamic mesh to analyze the growth and movement of multiple dendrites in binary alloy under melt convection. The results show that the established model can deal with the problem of morphology preservation well in the process of dendrite movement. Zhu et al. [7] simulated the growth of Fe-C alloy based on the established PF-LB model and accelerated the established model through parallel computing. Among them, CA and PF methods are most commonly used to simulate dendrite growth. However, there are some defects in quantitative simulation using the CA method. The main reason is that the method needs to keep track of the solid-liquid interface continuously during the calculation process. In addition, the anisotropy of the solid-liquid interface is affected dramatically by the grid. PF method can solve these problems well, so it has become the most popular method for dendrite growth simulation.

The Phase Field method has been widely used in various fields of material simulation in recent years. Hötzer et al. [8] used the Phase Field model to describe the microstructure evolution during solid-state sintering. Park et al. [9] researched the microstructure evolution of AlSi10Mg alloy using phase field simulation. Xing et al. [10] used the Phase Field model to study the competitive growth of columnar dendrites during directional solidification. Takaki et al. [11] applied the PF-LBM model to simulate the growth and movement of multiple dendrites. The results show that the established model is consistent with the theoretical research. Zhang et al. [12] used the PF-LBM method to simulate dendrite growth under convection and combined the adaptive mesh refinement method with parallel computing to improve the computational efficiency. However, there is an apparent defect in the above research on the calculation process of the phase-field model. That the quasi-phase equilibrium equation needs to be solved in each time step in the traditional phase-field model calculation process, and the solution step needs to be calculated at each grid, which increases the time cost significantly.

With the development of artificial intelligence, machine learning and deep learning methods have been widely used in material simulation research. Compared with traditional computing methods, machine learning and deep learning methods can learn the features contained in data automatically. In addition, the methods based on machine learning and deep learning also have the advantages of low computational overhead, high prediction accuracy and fast fitting speed that traditional methods do not have. Raccuglia et al. [13] used a large amount of data to train the machine learning model and predicted the reaction results of vanadium selenite crystallization. The results show that the machine learning model achieves an accuracy rate of 89%. Li et al. [14] proposed an approach based on high-throughput simulation combined with machine learning to analyze the best chemical-elemental composition in medium/high entropy alloys. Altay et al. [15] used Linear regression (LR), Support Vector Machine (SVM) and Gaussian Process Regression (GPR) methods to predict the wear loss quantities of ferroalloy coating. The prediction accuracy of the GPR and SVM models

could reach 96%. Kostiuchenko et al. [16] used the method based on machine learning models to study phase stability and phase transition and revealed the importance of local relaxation effect. Koenuma et al. [17] trained a deep learning model to fit the stress-strain curve of aluminum alloy sheets quickly. The experimental results show that the model trained by the neural network can predict the relevant parameters efficiently.

In the studies of phase field simulation using machine learning and deep learning methods, Teichert et al. [18] discussed the feasibility of using machine learning methods to detect the equilibrium state in physical systems. Montes de Oca Zapiain et al. [19] combined neural networks with the statistical data of microstructure evolution obtained from phase field simulation and predicted the microstructure of phase field models. Jiang et al. [20] proposed a method to apply machine learning models to predict quasi-phase equilibrium components based on the characteristics of quasi-phase equilibrium solutions. However, most of the existing applications of machine learning and deep learning methods in the material simulation are to predict the composition of alloy elements or to find new materials. Meanwhile there is relatively little research in numerical simulation of phase field method, and the accuracy of the prediction of aligned phase equilibrium is limited.

To solve the above problems, this paper takes Al-Cu-Mg ternary alloy as an example and builds the phase field model to simulate the microstructure formation during the solidification of dendrites. The study analyzes the dendrite morphology and solute field distribution of multiple dendrites under the competition and interaction. This work trains several machine learning and deep learning models to fit the prediction process of quasi-phase equilibrium components in the phase field model. The experimental results show that the proposed models can fit the quasi-phase equilibrium calculation accurately in the process of dendrite solidification well.

2 Numerical Methods

This study establishes the KKS [21] phase field model by using the method of regular solution to define the free energy. After coupling the free energy density to the thermodynamic database, it can be written as:

$$f(\varphi, c_1, c_2) = \left[h(\varphi) G_S^{reg} + (1 - h(\varphi)) G_L^{reg}\right] / V_m + Wg(\varphi) \tag{1}$$

$$h(\varphi) = \varphi^3 \left(10 - 15\varphi + 6\varphi^2\right) \tag{2}$$

$$g(\varphi) = \varphi^2 (1 - \varphi)^2 \tag{3}$$

where V_m represents the molar volume, W represents the double-well potential height, and φ represents the phase field parameter. The Gibbs free energy of each phase in the multicomponent alloy is related to the solution of related thermodynamic parameters. For ternary alloys, liquid and solid phases Gibbs free energy G_L^{reg} and G_S^{reg} can be described as:

$$G_L^{reg} = \sum_{i=1}^{3} \left(c_{iL}\mu_{iL}^0 + RTc_{iL} \ln c_{iL}\right) + G_L^{ex} \tag{4}$$

$$G_S^{reg} = \sum_{i=1}^{3} \left(c_{iS}\mu_{iS}^0 + RTc_{iS} \ln c_{iS}\right) + G_S^{ex} \tag{5}$$

where L represents the liquid phase, S represents the solid phase, c represents the solute concentration, $i = 1, 2$ in the subscript represents solute component 1 or solute component 2 and $i = 3$ in the subscript represents the solvent component. μ_{iL}^0 and μ_{iS}^0 represent the liquid and solid phase chemical potentials in the normal state, respectively. R represents the gas constant, and T represents the temperature. The

residual free energy G_L^{ex} and G_S^{ex} of Al-Cu-Mg ternary alloy can be expressed as [22]:

$$G_L^{ex} = c_3c_1\left[(-66622+8.1T)+(46800-90.8T+10TlnT)(c_3-c_1)-2812(c_3-c_1)^2\right]+ c_3c_2[(-12000+8.566T)+(1894-3T)(c_3-c_2)+2000(c_3-c_2)^2]+c_1c_2[(-36984+ 4.7561T)-8191.29(c_1-c_2)] \tag{6}$$

$$G_S^{ex} = c_3c_1[(-53520+2T)+(38590-2T)(c_3-c_1)-1170(c_3-c_1)^2]+c_3c_2[(4971- 3.5T)+(900+0.423T)(c_3-c_2)+950(c_3-c_2)^2]+c_1c_2(-22279.28+5.868T) \tag{7}$$

where c_1, c_2 and c_3 represent the concentrations of Cu, Mg and Al, respectively.

The phase field control equation during simulation can be expressed as:

$$\frac{\partial\varphi}{\partial t} = M\left(\varepsilon^2\nabla^2\varphi - f_\varphi\right) \tag{8}$$

where f_φ represents the first derivative of the free energy density to the phase field, M represents the phase field mobility. In addition, ε represents a parameter related to the interface energy, and the value is expressed by the following formula:

$$\varepsilon(\theta_i) = \varepsilon_0(1+\nu\cos(k\theta_i)) \tag{9}$$

$$\varepsilon_0 = \sqrt{\frac{6\lambda\sigma}{2.2}} \tag{10}$$

where σ represents the interface energy, θ represents the angle between the x-axis and the preferred growth direction of grains, subscript i represents a particular grain, and k represents the symmetry coefficient, which is set to 4 in the actual calculation of the phase field model, λ represents a parameter related to the interface thickness. θ is defined as follows:

$$\theta_i = \frac{\gamma_i\pi}{2} + \arctan\frac{\phi_y}{\phi_x}\ (i=1,2,\ldots,n) \tag{11}$$

where γ_i represents a random number from 0 to 1. ϕ_x and ϕ_y represent the partial derivatives of the phase field in the x and y axes, respectively. When the method of non-uniform nucleation is adopted, seeds are distributed randomly in the simulation area, and the number of seeds is a random number less than the maximum number of nucleation. The maximum nucleation number is calculated by the nucleation density. The variation of nucleation density follows a Gaussian distribution in the model:

$$\frac{dn}{d(\Delta T)} = \frac{n_{max}}{\sqrt{2\pi}\Delta T_\sigma}\exp\left(-\frac{(\Delta T-\Delta T_{max})^2}{2\Delta T_\sigma^2}\right) \tag{12}$$

where ΔT represents the degree of undercooling, n_{max} represents the maximum nucleation density, ΔT_σ represents the standard deviation undercooling, and ΔT_{max} represents the maximum nucleation undercooling.

The solute field control equation used in the simulation is expressed as:

$$\frac{\partial c_i}{\partial t} = \nabla\left(h(\varphi)\sum_{j=1}^{2}D_{ij}^S\nabla c_{iS} + (1-h(\varphi))\sum_{j=1}^{2}D_{ij}^L\nabla c_{iL}\right) \tag{13}$$

where D_{ij}^S and D_{ij}^L are solute diffusion coefficients in the solid and liquid phases, respectively. When the two phases are balanced, there is a constraint between the equilibrium component c_{iL} and c_{iS} at every point [23]:

$$c_i = h(\varphi)\, c_{iS} + (1 - h(\varphi))\, c_{iL} \quad (i = 1, 2) \tag{14}$$

$$\partial G_S^{reg}(c_{1S}, c_{2S})/\partial c_{iS} = \partial G_L^{reg}(c_{1L}, c_{2L})/\partial c_{iL} \tag{15}$$

During the simulation, the single-phase field controls multiple seeds by Eqs. (9) and (11). The coordinates of the seeds in the grid are randomly given. The number of seeds is determined by Eq. (12). Eqs. (8) and (13) are the phase field governing equation and solute field governing equation in the simulation process, respectively. Eqs. (14) and (15) are the quasi-phase equilibrium calculation equations in the phase field model.

3 Machine Learning and Deep Learning

This section introduces the experimental settings and related methods involved in the quasi-phase equilibrium prediction of the Kim-Kim-Suzuki (KKS) phase field model combining machine learning and deep learning methods.

3.1 Calculation Condition Setting

This work takes Al-Cu-Mg ternary alloy as an example to establish the KKS phase field model. In the undercooling liquid, the content of Cu (solute 1) is 2%, and the content of Mg (solute 2) is 3.5%. The physical parameters required in the simulation process are shown in Table 1.

Table 1: Physical parameters

Property	Value
Interfacial energy σ	$0.093\ \mathrm{J \cdot m^{-2}}$
Melting temperature T_m	930 K
Diffusion coefficient of Cu in solid phase	$10^{-5}\ exp\,(-16104/T)$
Diffusion coefficient of Cu in liquid phase	$1.06 \times 10^{-7}\ exp\,(-2887/T)$
Diffusion coefficient of Mg in solid phase	$0.37\ exp\,(-14854/T)$
Diffusion coefficient of Mg in liquid phase	$9.9 \times 10^{-5}\ exp\,(-8610/T)$
Molar volume	1.06×10^{-5}

The study obtains a large amount of data in the simulation process and uses the data to establish the model, which can predict the quasi-phase equilibrium in the phase field model. The study uses a single NVIDIA GeForce RTX 2060 GPU to train the model. Machine learning models are implemented using Scikit-learn, and deep learning models are implemented using the TensorFlow. As the prediction of the quasi-phase equilibrium can be regarded as a regression task, the paper uses Mean Squared Error (MSE) and Mean Absolute Error (MAE) as the evaluation criteria of the proposed methods. All deep learning models use the Adam optimizer to train 50 epochs, and the parameters of the models are determined by grid search based on the evaluation criteria of the models.

Fig. 1 shows the research process of the quasi-phase equilibrium prediction model established in this paper. This paper combines Eqs. (6), (7), (14) and (15) in the data preparation stage to solve the quasi-phase equilibrium of the phase field model. $c_i (i = 1, 2)$ and φ are combined as independent variables. c_{iL} and $c_{iS} (i = 1, 2)$ are used as dependent variables. This paper uses $\{c_1, c_2, \varphi\}$ as the input of models, and uses $\{c_{1L}, c_{2L}, c_{1S}, c_{2S}\}$ as the output of models. To verify the reliability of the model, this paper divides the data set containing 499900 pieces of data into the training set, validation set and

test set according to the ratio of 8:1:1. Firstly, the study trains the models on the training set, and then determine the optimal parameters of models on the validation set. Finally, the quasi-phase equilibrium prediction performance of the KKS phase field model is analyzed through the results of the trained model on the test set. This study mainly fits the prediction process of the aligning phase equilibrium according to the established KKS model. In addition, the required independent variables $\{c_1, c_2\}$ are obtained by selecting randomly between the solidus and the liquidus at the isotherm interface under the condition of 630°C. The independent variable $\{\varphi\}$ is obtained by randomly selecting a value between 0 and 1.

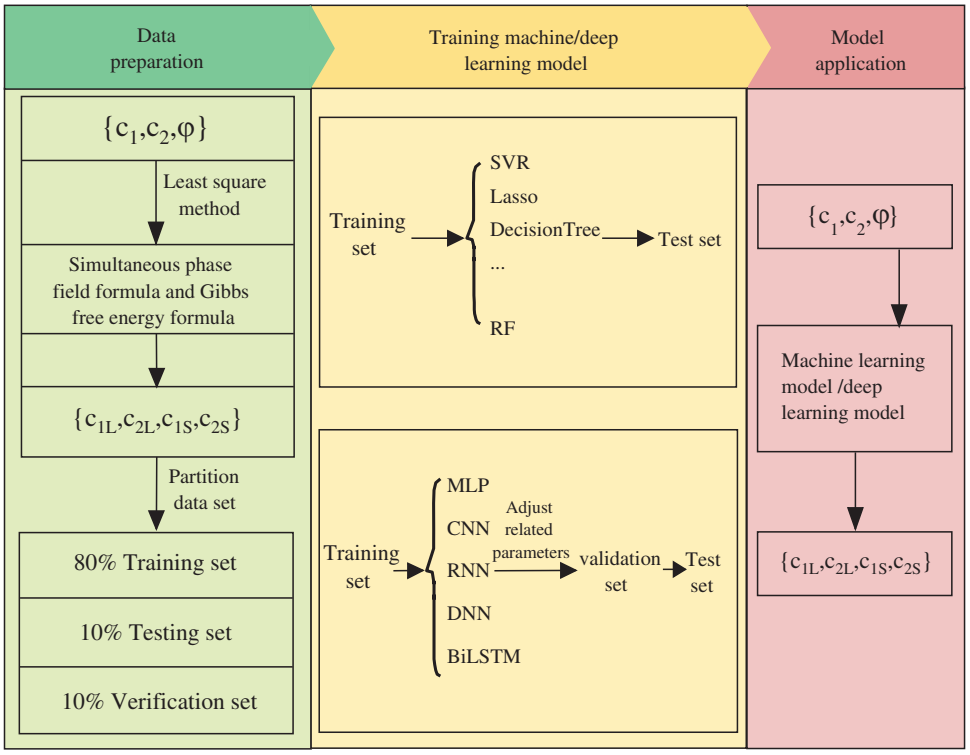

Figure 1: Overall research process

3.2 Machine Learning Methods

This study applies the following eight machine learning methods to predict the quasi-phase equilibrium of the multicomponent alloy KKS phase field model. It compares the prediction performance and effectiveness of these methods:

- Support Vector Regression (SVR) [24]: SVR is a supervised learning algorithm. The method regards all the data as a class and minimizes the intraclass variance of all the data through training. One of the main advantages of SVR is that the computational complexity does not depend on the dimensions of the input space. In addition, the method has excellent generalization ability and high prediction accuracy.
- Decision tree (DT) [25]: The Decision tree is a supervised machine learning method which can summarize decision rules from a series of characteristic data. In constructing the decision tree, the sample search is performed according to the values of different levels of the decision tree, the

corresponding leaf-level sub-table is selected, and the output result of this leaf-level sub-table is used as the result of the predicted sample.

- Linear regression (LR) [26]: The goal of linear regression is to predict the linear combination of input variables. That the linear function is used to fit the known data and further predict the unknown data.
- Ridge regression (RR) [27]: The essence of ridge regression is an improved least square estimation method. The method obtains a more realistic and reliable regression method at the expense of losing some information and reducing accuracy. It fits ill-conditioned data better than least squares.
- Lasso [28]: Lasso regression model is characterized by variable selection and complexity regularization while fitting the generalized linear model, in which complexity adjustment refers to controlling the complexity of the model through a series of parameters to avoid overfitting. Therefore, Lasso is an effective biased estimation method.
- Random Forest (RF) [29]: Random Forest is composed of multiple decision trees, each of which is different. Random forest applies the Bagging algorithm to integrate the advantages of multiple base models. Random forest is not prone to over-fitting, has strong anti-noise ability and can handle high-dimensional data with many features.
- ExrRa Trees (ET) [30]: Similar to the random forest algorithm, the ExrRa Trees method is generally applied to large-scale data. The difference from the random forest is that all training samples are applied to each decision tree. After selecting the partition characteristics, the ExrRa Trees method gets the best partition point in a entirely unexpected way.
- Adaboost [31]: AdaBoost method is an iterative integration algorithm. A new weak model is added in each round until a predetermined error rate is low enough. Compared with the other machine learning models, the AdaBoost method can focus on the samples that are difficult to distinguish.

3.3 Deep Learning Methods

This paper uses the following five deep learning models to complete the prediction experiment of the quasi-phase equilibrium equation:

- Multilayer Perceptron (MLP) [32]: MLP can be seen as a directed graph composed of multiple layers, and each layer is connected to the next layer, that is, layers of MLP are full-connection, and include an input layer, an output layer and one or more hidden layers in the middle. The mechanism is equivalent to a single-layer neural network with one hidden layer, where the output of hidden layers is transformed by the activation function. This work uses 4 full-connection layers with output dimensions of 16,64,128 and 1 to extract features and get the prediction results.
- Convolutional Neural Network (CNN) [33]: CNN is a standard deep learning model, which was first applied to computer vision. This paper uses a one-dimensional convolution layer with 16 convolution kernels of size 1 to extract the features contained in the data. Then the work obtains the final regression prediction result after the max-pooling layer and the full-connection layer.
- Recurrent Neural Network (RNN) [34]: RNN has the characteristics of memory and parameter sharing, so it has certain advantages in learning the nonlinear characteristics of sequences. When applied to the training of quasi-phase equilibrium prediction, the study embeds the original data into the 64-dimensional feature space firstly by using the embedding layer, then extracting the features by using simple RNN with the 80-dimensional hidden layer and setting the dropout to 0.2. Finally, this study obtains the prediction results by the full-connection layer.

- Deep Neural Network (DNN) [35]: DNN is equivalent to MLP model with multiple hidden layers. The advantage is that solid nonlinear fitting ability. This study uses the flatten layer to flatten the input data and 20 full-connection layers to extract features.
- Bi-directional Long Short-term Memory (BiLSTM) [36]: BiLSTM can solve the long-term dependence problem in RNN. BiLSTM is composed of forward LSTM and backward LSTM, and the prediction process is jointly determined by the features extracted by the two LSTM models. This study uses two LSTM models with 64-dimensional output dimensions to extract features and then obtain the regression prediction results.

4 Results and Discussion

This paper establishes the quasi-phase equilibrium prediction of the phase field model, and the process is a regression problem in essence. The paper evaluates the performance of the trained model comprehensively by utilizing MSE and MAE. The specific expressions of MSE and MAE are defined as follows:

$$MSE\,(y, y') = \frac{1}{n}\sum_{i=1}^{n}\left(y_i - y_i'\right)^2 \tag{16}$$

$$MAE\,(y, y') = \frac{1}{n}\sum_{i=1}^{n}\left|\left(y_i - y_i'\right)\right| \tag{17}$$

where y_i represents the real value calculated by the least square method, and y_i' represents the value predicted by the machine learning or deep learning model. The range of MSE and MAE is $(0, +\infty)$, and the bigger its value, the bigger the error of the trained model. In the measurement process, MSE is more accessible to calculate than MAE, while MSE amplifies the influence of outliers on the model, and MAE has better robustness to outliers.

4.1 The Result of the KKS Model Simulation

Based on the KKS phase field model, this paper simulates the growth process of Al-Cu-Mg ternary alloy in this paper. Fig. 2 shows the simulation results of multiple grains growing together.

Fig. 2a shows the morphology of multiple dendrites growing together. Taking dendrite M as an example, it can be seen from Fig. 2 that multiple dendrites compete for growth at this time, which results in mutual influence. Due to the influence of other dendrite arms, the main dendrite arm in the upward left part of dendrite M would not grow straight while leaning downward. Meanwhile, the main dendrite arm in the upward right part of dendrite M is squeezed, which leads to growth in the upward left position. The morphology of dendrite M is deformed by the other dendrite arms' action. In the direction of dendrite as contact with other dendrites, the growth of dendrite M's dendrite arms is restrained, which results in relatively thinner dendrite arms. In the non-contact direction, the growth of dendrite arms is not restricted, and the shapes of primary and secondary dendrite arms are thicker. Figs. 2b and 2c show the solute field distribution of Cu and Mg, respectively. It can be seen from the simulation results that solute elements are enriched in the gaps between the main dendrite arm and the secondary dendrite arm of the five dendrites due to solute redistribution in the solidification process of the microstructure.

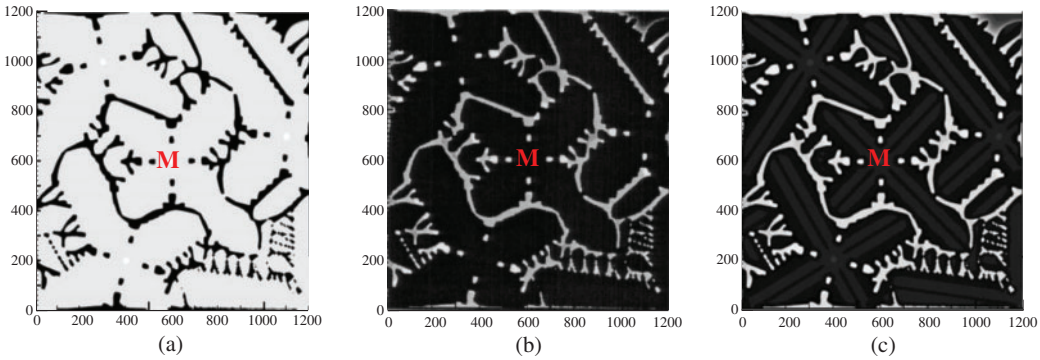

Figure 2: Simulation results of co-growth of multiple grains: (a) morphology of co-growth of multiple dendrites; (b) solute field distribution of Cu; (c) solute field distribution of Mg

4.2 Analysis of Machine Learning Prediction Results

According to the experimental setup introduced in Section 3.1, this paper uses different machine learning methods to train quasi-phase equilibrium prediction models and measure the models by MSE and MAE. Table 2 shows the comparison of regression results of different machine learning models. Adaboost achieves competitive performance in the prediction results of each quasi-phase equilibrium component. Compared with other methods, the prediction result of c_{1L} is the best, with MSE and MAE reaching 0.0010455 and 0.0272086, respectively. In addition, the LR method achieves the lowest mean square error in the prediction of quasi-phase equilibrium components c_{1S} and c_{2S}, and the values are 0.0000572 and 0.000444, respectively. While for the prediction results of quasi-phase equilibrium components c_{2L} and c_{2S}, the RR is the best algorithm, which MAE values are 0.0114369 and 0.0049593, respectively.

Table 2: Comparison of regression results of machine learning methods

Method	Standard	c_{1L}	c_{2L}	c_{1S}	c_{2S}
SVR	MSE	0.0026994	0.0022303	0.0003254	0.0003949
	MAE	0.0455463	0.0408023	0.0167022	0.0176205
DT	MSE	0.0020415	0.0004560	0.0001146	0.0000858
	MAE	0.0327152	0.0138982	0.0069760	0.0059948
ET	MSE	0.0020409	0.0004531	0.0001163	0.0000874
	MAE	0.0326879	0.0138549	0.0070358	0.0060385
Lasso	MSE	0.0021202	0.0012138	0.0000917	0.0001676
	MAE	0.0386932	0.0285273	0.0074269	0.0103952
RR	MSE	0.0010787	0.0002433	**0.0000572**	0.0000445
	MAE	0.0276293	**0.0119816**	0.0057261	**0.0049952**
LR	MSE	0.0010785	0.0002432	**0.0000572**	**0.0000444**
	MAE	**0.0275964**	0.0119704	0.0057215	0.0049910
AdaBoost	MSE	**0.0010455**	**0.0002415**	0.0000587	0.0000452
	MAE	0.0272086	0.0120719	**0.0059084**	0.0051149
RF	MSE	0.0011839	0.0002630	0.0000663	0.0000503
	MAE	0.0272357	0.0114369	0.0058377	0.0049593

In general, RR, LR and AdaBoost models have good prediction results after training, which may be because that RR is an improved least square estimation method, and it performs better in the analysis of collinear data. The significant performance of LR may be due to the robustness of small noise data, and it would not be affected by multicollinearity greatly when applied to large data sets. AdaBoost adopts the idea of ensemble learning and achieves good results through continuous iteration in the training process. Among all machine learning methods, SVR achieves the worst performance in predicting the components of each quasi-phase equilibrium equation. This may be because the data set used in this study contains numerous samples, and SVR is unsuitable when the sample size is huge. In addition, the prediction of the quasi-phase equilibrium equation in this study is a nonlinear problem. There is no general standard for the kernel function selection of SVR in solving nonlinear problems, so it is hard to select a suitable kernel function.

4.3 Analysis of Deep Learning Prediction Results

To compare with machine learning methods, this study applies five deep learning methods proposed in Section 3.2 to the prediction of quasi-phase equilibrium. The experimental results are shown in Table 3. The results show that the application of deep learning methods to the prediction of quasi-phase equilibrium is generally better than machine learning. Among them, the MLP model shows the best performance, with the lowest MSE in predicting the four components. This is because the MLP model has self-adaptive and self-learning functions, which can learn the characteristics of the quasi-phase equilibrium equation data fully obtained in this study. In addition, the CNN model also achieves competitive results, and the MAE performance reaches 0.0262871 in the prediction result of c_{1L}, which is even better than the MLP model with generally better performance. CNN is the most commonly used deep learning model for feature extraction, and the fewer weights and lower network complexity make it well applied to phase-field model prediction simulation.

Table 3: Comparison of regression results of deep learning methods

Method	Standard	c_{1L}	c_{2L}	c_{1S}	c_{2S}
MLP	MSE	**0.0010150**	**0.0002244**	**0.0000568**	**0.0000430**
	MAE	0.0263096	**0.0110073**	**0.0056159**	**0.0047784**
CNN	MSE	0.0010157	0.0002278	0.0000577	0.0000443
	MAE	**0.0262871**	0.0112286	0.0056303	0.0048464
RNN	MSE	0.0021205	0.0012138	0.0000918	0.0001676
	MAE	0.0387410	0.0285452	0.0073480	0.0103913
BiLSTM	MSE	0.0010151	0.0002250	0.0000573	0.0000431
	MAE	0.0263662	0.0110726	0.0056605	0.0048271
DNN	MSE	0.0010168	0.0002277	**0.0000568**	0.0000438
	MAE	0.0263058	0.0110619	0.0056277	0.0047982

Among all the deep learning methods, RNN performs poorly under the two evaluation criteria. The reason may be that RNN connects neurons serially in the training process, requiring previous

knowledge and experience to deal with the subsequent steps. Therefore, the model is more suitable for dealing with timing problems but not for this study. However, the BiLSTM model, which is similar to the RNN structure, performs better than the RNN model. Because BiLSTM solves the long-term dependence problem in RNN, and the prediction process of the model is determined by the features extracted by two LSTM models, which weakens the influence of neuron sequence.

In addition, this paper compares the prediction results of machine learning and deep learning methods under MSE and MAE standards, and the results are shown in Figs. 3 and 4, respectively. The orange reference line, green reference line, purple reference line and yellow reference line in Figs. 3 and 4 show the best results achieved in the prediction of c_{1L}, c_{2L}, c_{1S} and c_{2S}, respectively. It can be seen from Fig. 3 that when applies several machine learning and deep learning methods to the prediction of quasi-phase equilibrium, the prediction results of c_{1S} and c_{2S} are better than those of c_{1L} and c_{2L}, and the results of deep learning methods are better than those of machine learning methods. When the MLP model is adopted, the MLP model-based quasi-phase equilibrium prediction of c_{1L}, c_{2L}, c_{1S} and c_{2S} is the best, and DNN and BiLSTM can also achieve significant results. Fig. 4 shows an overall trend similar to that of Fig. 3, which shows that deep learning methods are more suitable for the quasi-phase equilibrium prediction of the phase field model proposed in this paper than machine learning. Compared with the classical machine learning methods, deep learning models can learn the features contained in the data more fully and automatically. Compared with the Adaboost method, which performs better in machine learning, deep learning methods such as MLP use fewer training epochs and get better performance. In addition, although the same methods are applied to predicting different quasi-phase equilibria, the prediction results are also very different. For example, the MSE of Lasso on c_{1S} has a little deviation from the best value, while the MSE of Lasso on c_{1L} has a significant deviation from the best value. In contrast, the prediction results of the four components of the CNN model are all close to the best results. That is, the mobility and robustness of the Lasso method are lower than those of CNN when applied to the quasi-phase equilibrium prediction of the phase field model.

It can be seen from Figs. 3 and 4 that the prediction results of the other four deep learning methods for c_{1L}, c_{2L}, c_{1S} and c_{2S} are approximately close to four reference lines except for RNN, which means the overall performance of deep learning models are better than those of machine learning methods. In general, the quasi-phase equilibrium prediction of the MLP model achieves the best performance, whether measured by MAE or MSE standard.

Fig. 5 shows the changing loss trend on the training and validation set for four different outputs during training the MLP model. To show the training effect of the model more intuitively, this paper trains 200 epochs with the best MLP model. It can be seen from the downward trend of loss that the model achieves a relatively stable loss after 25 epochs of training, and the trained model does not produce serious over-fitting. It can be seen from Figs. 5a and 5b that when the model is trained for about ten epochs, the declining trend of loss begins to flatten, which means a prediction model with good performance can be obtained through about ten epochs of training. However, the curves in Figs. 5c and 5d show a specific oscillation phenomenon during the training and validation process. This may be because of a certain amount of noise in the train set data.

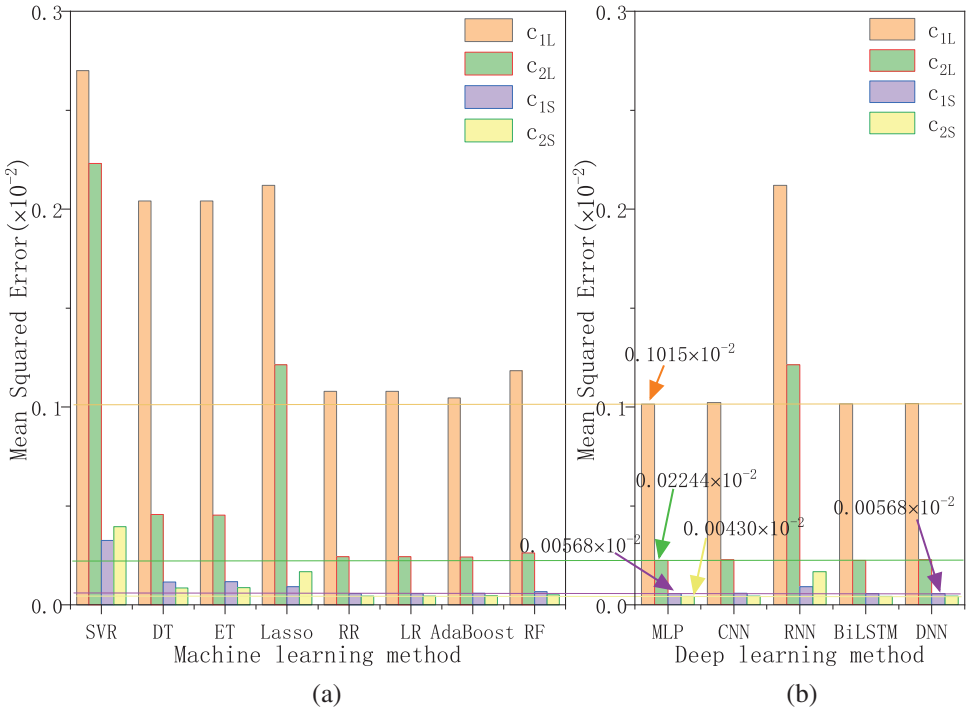

Figure 3: Comparison between machine learning and deep learning methods under MSE standard

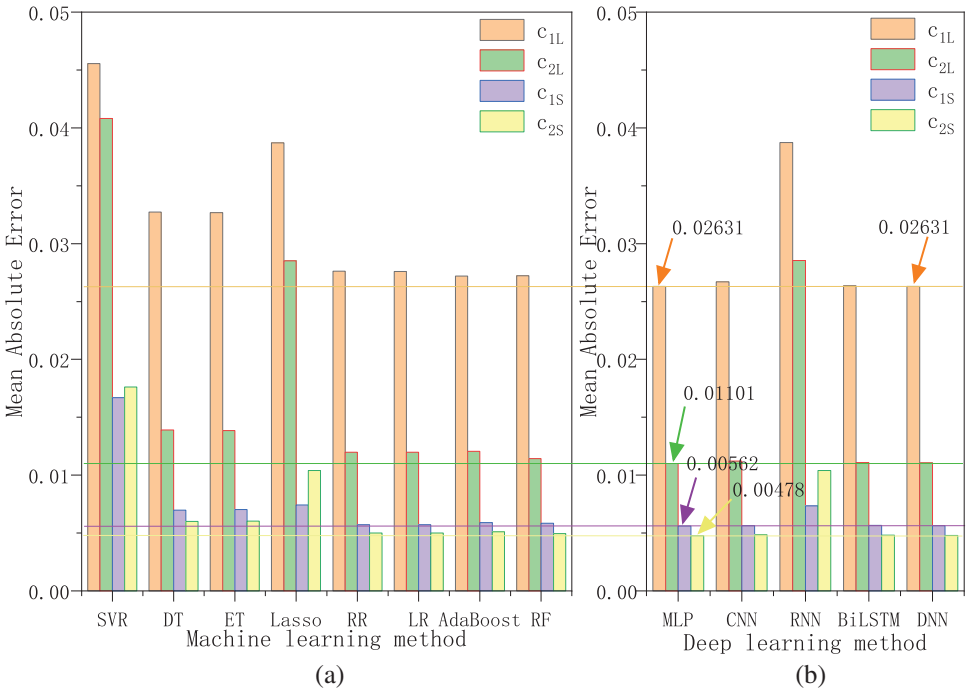

Figure 4: Comparison between machine learning and deep learning methods under MAE standard

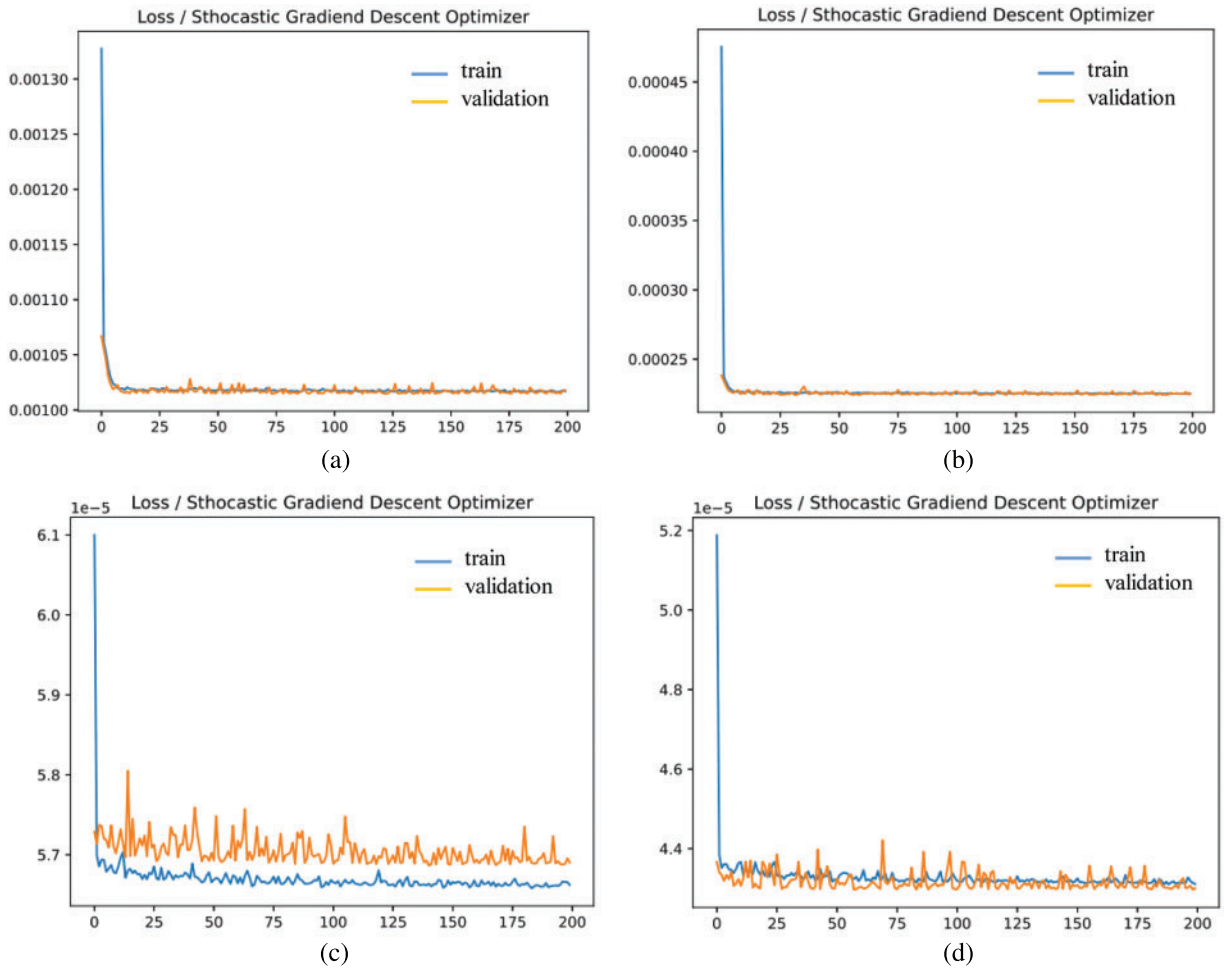

Figure 5: Change trend of training and validation loss during MLP training

5 Conclusion

This study takes Al-Cu-Mg ternary alloy as the research object, establishes the KKS model and studies the prediction of quasi-phase equilibrium by combining different machine learning and deep learning methods. The conclusions are as follows:

(1) This paper couples KKS phase field model with the solute field and simulates the morphology of multiple dendrites growing together. The results show that the growth of multi-grains will lead to the interaction between dendrite arms. Based on the quasi-phase equilibrium equation in the KKS model, this study obtains 499900 pieces of quasi-phase equilibrium data and trains the model by this data set.

(2) This paper predicts the quasi-phase equilibrium using machine learning methods. The results show that the performance of prediction models trained by different machine learning methods is significant basically. Meanwhile, SVR is not suitable for the quasi-phase equilibrium prediction of the KKS model proposed in this paper. In addition, RR, LR and AdaBoost

methods have relatively excellent prediction results, which are consistent with the prediction of quasi-phase equilibrium of the KKS model.

(3) In this study, different deep learning methods are further applied to the data set, and the results are evaluated according to MSE and MAE standards. The results show that the performance of the models trained by deep learning methods is better than that of the models trained by machine learning, among which the quasi-phase equilibrium prediction model based on MLP shows the best performance.

(4) In this study, machine learning and deep learning methods are used to fit the quasi-phase equilibrium calculation in the phase-field simulation process, which proves that the combination of machine learning, deep learning and phase-field simulation is feasible and effective. Furthermore, this paper finds that machine learning and deep learning models have significant advantages in simulating dendrite growth morphology and predicting alloy properties in combination with phase-field simulation. The future work will focus on the application of machine learning and deep learning methods for dendrite growth simulation.

Funding Statement: This work is supported by the National Natural Science Foundation of China under Grant Nos. 52161002, 51661020 and 11364024.

Conflicts of Interest: The authors declare that they have no conflicts of interest to report regarding the present study.

References

[1] V. Kumar, A. Srivastava and S. Karagadde, "Role of microstructure and composition on natural convection during ternary alloy solidification," *Journal of Fluid Mechanics*, vol. 913, no. 1, pp. A41-1–A41-29, 2021.

[2] D. Sun, M. Zhu, S. Pan and D. Raabe, "Lattice Boltzmann modeling of dendritic growth in a forced melt convection," *Acta Materialia*, vol. 57, no. 6, pp. 1755–1767, 2009.

[3] M. Eshraghi, S. D. Felicelli and B. Jelinek, "Three dimensional simulation of solutal dendrite growth using lattice Boltzmann and cellular automaton methods," *Journal of Crystal Growth*, vol. 354, no. 1, pp. 129–134, 2012.

[4] R. Chen, Q. Xu and B. Liu, "Cellular automaton simulation of three-dimensional dendrite growth in Al–7Si–Mg ternary aluminum alloys," *Computational Materials Science*, vol. 105, no. 10, pp. 90–100, 2015.

[5] S. Sakane, T. Takaki, R. Rojas, M. Ohno, Y. Shibuta *et al.,* "Multi-GPUs parallel computation of dendrite growth in forced convection using the phase-field-lattice Boltzmann model," *Journal of Crystal Growth*, vol. 474, no. 1, pp. 154–159, 2017.

[6] S. Zhang, C. Li and R. Li, "Cellular automata-lattice Boltzmann simulation of multi-dendrite motion under convection based on dynamic grid technology," *Materials Today Communications*, vol. 31, no. 2, pp. 103342, 2022.

[7] C. S. Zhu, Y. J. Li, F. L. Ma, L. Feng and P. Lei, "Three-dimensional multi-phase-field simulation of eutectoid alloy based on OpenCL parallel," *China Foundry*, vol. 18, no. 3, pp. 239–248, 2021.

[8] J. Hötzer, M. Seiz, M. Kellner, W. Rheinheimer and B. Nestler, "Phase-field simulation of solid state sintering," *Acta Materialia*, vol. 164, no. 3, pp. 184–195, 2019.

[9] J. Park, J. H. Kang and C. S. Oh, "Phase-field simulations and microstructural analysis of epitaxial growth during rapid solidification of additively manufactured AlSi10Mg alloy," *Materials & Design*, vol. 195, no. 11, pp. 108985, 2020.

[10] H. Xing, M. Ji, X. Dong, Y. Wang, L. Zhang *et al.,* "Growth competition between columnar dendrite and degenerate seaweed during directional solidification of alloys: Insights from multi-phase field simulations," *Materials & Design*, vol. 185, no. 1, pp. 108250, 2020.

[11] T. Takaki, R. Sato, R. Rojas, M. Ohno and Y. Shibuta, "Phase-field lattice Boltzmann simulations of multiple dendrite growth with motion, collision, and coalescence and subsequent grain growth," *Computational Materials Science*, vol. 147, no. 7, pp. 124–131, 2018.
[12] X. Zhang, J. Kang, Z. Guo, S. Xiong and Q. Han, "Development of a para-AMR algorithm for simulating dendrite growth under convection using a phase-field–lattice Boltzmann method," *Computer Physics Communications*, vol. 223, no. 2, pp. 18–27, 2018.
[13] P. Raccuglia, K. C. Elbert, P. D. Adler, C. Falk, M. B. Wenny *et al.,* "Machine-learning-assisted materials discovery using failed experiments," *Nature*, vol. 533, no. 7601, pp. 73–76, 2016.
[14] J. Li, B. Xie, Q. Fang, B. Liu, Y. Liu *et al.,* "High-throughput simulation combined machine learning search for optimum elemental composition in medium entropy alloy," *Journal of Materials Science & Technology*, vol. 68, no. 9, pp. 70–75, 2021.
[15] O. Altay, T. Gurgenc, M. Ulas and C. Özel, "Prediction of wear loss quantities of ferro-alloy coating using different machine learning algorithms," *Friction*, vol. 8, no. 1, pp. 107–114, 2020.
[16] T. Kostiuchenko, F. Körmann, J. Neugebauer and A. Shapeev, "Impact of lattice relaxations on phase transitions in a high-entropy alloy studied by machine-learning potentials," *npj Computational Materials*, vol. 5, no. 1, pp. 1–7, 2019.
[17] K. Koenuma, A. Yamanaka, I. Watanabe and T. Kuwabara, "Estimation of texture-dependent stress-strain curve and r-value of aluminum alloy sheet using deep learning," *Materials Transactions*, vol. 61, no. 12, pp. 2276–2283, 2020.
[18] G. H. Teichert and K. Garikipati, "Machine learning materials physics: Surrogate optimization and multi-fidelity algorithms predict precipitate morphology in an alternative to phase field dynamics," *Materials Transactions*, vol. 344, no. 2, pp. 666–693, 2019.
[19] D. Montes de Oca Zapiain, J. A. Stewart and R. Dingreville, "Accelerating phase-field-based microstructure evolution predictions via surrogate models trained by machine learning methods," *npj Computational Materials*, vol. 7, no. 1, pp. 1–11, 2021.
[20] X. Jiang, R. Zhang, C. Zhang, H. Yin and X. Qu, "Fast prediction of the quasi phase equilibrium in phase field model for multicomponent alloys based on machine learning method," *Calphad*, vol. 66, no. 3, pp. 101644, 2019.
[21] S. G. Kim, W. T. Kim and T. Suzuki, "Phase-field model for binary alloys," *Physical Review e*, vol. 60, no. 6, pp. 7186, 1999.
[22] R. Zhang, T. Jing, W. Jie and B. Liu, "Phase-field simulation of solidification in multicomponent alloys coupled with thermodynamic and diffusion mobility databases," *Acta Materialia*, vol. 54, no. 8, pp. 2235–2239, 2006.
[23] S. G. Kim, "A phase-field model with antitrapping current for multicomponent alloys with arbitrary thermodynamic properties," *Acta Materialia*, vol. 55, no. 13, pp. 4391–4399, 2007.
[24] H. Drucker, C. J. Burges, L. Kaufman, A. Smola and V. Vapnik, "Support vector regression machines," in *NIPS*, Denver, CO, USA, MIT Press, pp. 155–161, 1996.
[25] M. Xu, P. Watanachaturaporn, P. K. Varshney and M. K. Arora, "Decision tree regression for soft classification of remote sensing data," *Remote Sensing of Environment*, vol. 97, no. 3, pp. 322–336, 2005.
[26] O. O. Aalen, "A linear regression model for the analysis of life times," *Statistics in Medicine*, vol. 8, no. 8, pp. 907–925, 1989.
[27] D. W. Marquardt and R. D. Snee, "Ridge regression in practice," *The American Statistician*, vol. 29, no. 1, pp. 3–20, 1975.
[28] C. Hans, "Bayesian lasso regression," *Biometrika*, vol. 96, no. 4, pp. 835–845, 2009.
[29] V. Svetnik, A. Liaw, C. Tong, J. C. Culberson, R. P. Sheridan *et al.,* "Random forest: A classification and regression tool for compound classification and QSAR modeling," *Journal of Chemical Information and Computer Science*, vol. 43, no. 6, pp. 1947–1958, 2003.
[30] P. Geurts, D. Ernst and L. Wehenkel, "Extremely randomized trees," *Machine Learning*, vol. 63, no. 1, pp. 3–42, 2006.

[31] M. Collins, R. E. Schapire and Y. Singer, "Logistic regression, AdaBoost and Bregman distances," *Machine Learning*, vol. 48, no. 1, pp. 253–285, 2002.
[32] F. Murtagh, "Multilayer perceptrons for classification and regression," *Neurocomputing*, vol. 2, no. 5–6, pp. 183–197, 1991.
[33] A. Krizhevsky, I. Sutskever and G. E. Hinton, "Imagenet classification with deep convolutional neural networks," *Communications of the ACM*, vol. 60, no. 6, pp. 84–90, 2017.
[34] W. Zaremba, I. Sutskever and O. Vinyals, "Recurrent neural network regularization," arXiv preprint arXiv:1409.2329, 2014.
[35] G. E. Hinton and R. R. Salakhutdinov, "Reducing the dimensionality of data with neural networks," *Science*, vol. 313, no. 5786, pp. 504–507, 2006.
[36] M. Schuster and K. K. Paliwal, "Bidirectional recurrent neural networks," *IEEE Transactions on Signal Processing*, vol. 45, no. 11, pp. 2673–2681, 1997.